

PAPER • OPEN ACCESS

Structure and magnetic properties of $(\text{Sm}_{1-x}\text{Zr}_x)\text{Fe}_{11}\text{Ti}$ ($x=0-0.2$) alloys

To cite this article: I Ryzhikhin *et al* 2019 *J. Phys.: Conf. Ser.* **1389** 012117

View the [article online](#) for updates and enhancements.



IOP | ebooks™

Bringing together innovative digital publishing with leading authors from the global scientific community.

Start exploring the collection—download the first chapter of every title for free.

Structure and magnetic properties of $(\text{Sm}_{1-x}\text{Zr}_x)\text{Fe}_{11}\text{Ti}$ ($x=0-0.2$) alloys

I Ryzhikhin, S Andreev, M Semkin, N Selezneva, A Volegov and N Kudrevatykh

Institute of Natural Sciences and Mathematics, Ural Federal University, 620002
Ekaterinburg, Russia

E-mail: ilya.ryzhikhin@urfu.ru

Abstract. Compounds with a tetragonal structure of the ThMn_{12} type have a high potential for creating on their basis permanent magnets with high energy density and operating temperatures up to 150 – 200 °C. In this work, samples of alloys $(\text{Sm}_{1-x}\text{Zr}_x)\text{Fe}_{11}\text{Ti}$ ($x = 0 - 0.2$) obtained by the rapidly quenching method with subsequent annealing were investigated. Depending on the chemical composition and modes of synthesis in alloys $(\text{Sm}_{1-x}\text{Zr}_x)\text{Fe}_{11}\text{Ti}$ ($x = 0 - 0.2$) phases of the ThMn_{12} , α -Fe type and a small amount of ZrFe_2 are formed, as well as phases with the $\text{Th}_2\text{Zn}_{17}$ structural type and TbCu_7 at high annealing temperatures. The best magnetic properties at room temperature are realized in the alloy $(\text{Sm}_{0.9}\text{Zr}_{0.1})\text{Fe}_{11}\text{Ti}$ after annealing at a temperature of 800 °C.

1. Introduction

The study of intermetallic compounds like RT_{12} (R is a rare-earth metal, T is a 3d-metal) with a ThMn_{12} -type structure has been occurring since the 1980's [1–3]. These compounds are considered promising for use as materials for the manufacturing of the permanent magnets due to the high value of the saturation magnetization (M_s) and the anisotropy field (H_a) [4]. The discovery of highly anisotropic $\text{Nd}_2\text{Fe}_{14}\text{B}$ compound and creating the production technology of permanent magnets based on the phase hampered the study of RFe_{12} compounds as a material for permanent magnets. The growing demand for magnets operating at 150 – 200 °C and the sharp rise in prices for rare earth metals in 2010 – 2011 triggered a study of magnets without rare-earth metals or magnetic materials with a lower content of rare earth metals including the already known RT_{12} . If RFe_{12} binary alloys were realized, they would have the highest Fe content among 4f-3d compounds and, thus, are expected to show the largest magnetization values and the maximum energy product.

The RFe_{12} phase is unstable and stabilizing additives are used for its formation, such as V, Mo, Nb, Al, etc. Moreover, depending on the stabilizing element (M), the number of its atoms varies from 0.5 to 8 per formula unit. Unlike $\text{Nd}_2\text{Fe}_{14}\text{B}$, compounds of the RFe_{12} type are characterized by a negative value of the crystal field parameter A_0^2 ; thus, they exhibit the strongest uniaxial magnetocrystalline anisotropy for rare-earth elements R with a positive second-order Stevens factor such as Sm [5]. It was reported [6] the atomic radius of the rare-earth element is an important factor for stabilizing the formation of a ThMn_{12} structure and Zr takes the place of Nd in $(\text{Nd}, \text{Zr})\text{Fe}_{10}\text{Si}_2$ systems and facilitates the formation of the ThMn_{12} -type phase due to a decrease in the atomic radius at the Nd site. By substitution a small amount of Sm by Zr in the compound $(\text{Sm}, \text{Zr})(\text{Fe}, \text{Co})_{11-y}\text{Ti}_y$ it



is possible to reduce the Ti content to 0.5 [7, 8]. Co additions leads to raise the Curie temperature which does not always occur in phases with a structure of the ThMn_{12} type [9, 10].

It is possible to obtain the ThMn_{12} type phase from an amorphous state by carrying out heat treatments $\text{RT}_{12-y}\text{M}_y$ [11,12].

In this paper, the crystal structure of $(\text{Sm}_{1-x}\text{Zr}_x)\text{Fe}_{11}\text{Ti}$ and its influence on the magnetic properties of these compounds with different Zr contents were investigated.

2. Experimental details

The alloys of the compositions $(\text{Sm}_{1-x}\text{Zr}_x)\text{Fe}_{11}\text{Ti}$ ($x = 0 - 0.2$) were obtained in an inert atmosphere by the induction melting from chemically pure elements (with a purity no worse than 99.9%). In the following, the synthesized alloys were melt spinning onto the outer surface of the copper disk in an inert atmosphere. Ribbons of alloys were heat treated under vacuum for 1 hour. The treatment temperature varied in the range of 500 – 1000 °C. The phase composition of samples of rapidly quenched alloys was investigated by X-ray diffraction analysis using a powder diffractometer (Bruker D8 Advance) in $\text{Cu K}\alpha$ radiation.

Temperature dependencies of the initial magnetic susceptibility were investigated by means of a custom-made susceptometer. Magnetic hysteresis properties were studied using vibration sample magnetometer in magnetic fields with an intensity of up to 25 kOe at room temperature. The demagnetizing factor of the samples was $N \approx 1.4 - 1.9$.

3. Results and discussion

Figure 1 presents the results of X-ray structural analysis (XRD) carried out for the $\text{SmFe}_{11}\text{Ti}$ alloys (figure 1a), $(\text{Sm}_{0.9}\text{Zr}_{0.1})\text{Fe}_{11}\text{Ti}$ (figure 1b) and $(\text{Sm}_{0.8}\text{Zr}_{0.2})\text{Fe}_{11}\text{Ti}$ (figure 1c) annealed at different temperatures.

The initial state of the alloy $(\text{Sm}_{0.9}\text{Zr}_{0.1})\text{Fe}_{11}\text{Ti}$ is characterized by a wide halo, which indicates its x-ray amorphous state. In the other two compositions, there are peaks of the crystalline phase Pt because of using corresponding substrate. According to the Sm-Fe binary phase diagram [13], for the stoichiometric composition of SmFe_{12} at room temperature, the $\text{Sm}_2\text{Fe}_{17}$ and $\alpha\text{-Fe}$ phases are equilibrium. However, in all samples which annealing temperature did not exceed 900 °C, there is no $\text{Sm}_2\text{Fe}_{17}$ type phase, the presence of a ThMn_{12} and $\alpha\text{-Fe}$ type was found.

The magnetic susceptibility vs. temperature of the alloys $(\text{Sm}_{1-x}\text{Zr}_x)\text{Fe}_{11}\text{Ti}$ (figure 2) annealed at different temperatures was studied. On the basis of these dependences, ferromagnetic phases precipitated in the alloys during the annealing process were determined. All alloys in the initial state contain an amorphous phase with a Curie temperature $T_C = 70 - 75$ °C and a small amount of the $\alpha\text{-Fe}$ phase. In the $\text{SmFe}_{11}\text{Ti}$ alloys (figure 2a), the ThMn_{12} type phase is also already present in the initial state. Also the $\chi(T)$ dependence demonstrate a peak at a temperature of 310 °C, which is close to the Curie temperature of the $(\text{Ti}, \text{Zr})\text{Fe}_2$ phase ($\text{Ti}_{0.75}\text{Zr}_{0.25}\text{Fe}_2$ has $T_C = 322$ °C). The presence of the $(\text{Ti}, \text{Zr})\text{Fe}_2$ phase was discussed in [12] for the $(\text{Sm}_{0.9}\text{Zr}_{0.1})\text{Fe}_{11}\text{Ti}$ alloy. In all the annealed samples, the $\alpha\text{-Fe}$ phase and the $(\text{Ti}, \text{Zr})\text{Fe}_2$ phase were detected. As the annealing temperature increases, crystallization of the amorphous phase occurs and the peak in the $\chi(T)$ dependence shifts to the value corresponding to the T_C phase of $\text{SmFe}_{11}\text{Ti}$ ($T_c = 327$ °C [14]). Figure 3 shows the dependence of the position of the maximum on T_a .

The linear growth of the position of the maximum of the magnetic susceptibility corresponding to T_C of major hard magnetic phase arising from the amorphous matrix occurs linearly with an increase of the annealing temperature. This growth is most likely due to an increase in the grain size of the hard magnetic phase of the ThMn_{12} type.

The hysteresis properties of the alloys were measured at different annealing temperatures. With an increase in T_a , an increase in H_C occurs, which is associated with an increase in the crystallite size of the main magnetic hard phase in the alloys (Figure 4). The maximum value of H_c has the composition $(\text{Sm}_{0.9}\text{Zr}_{0.1})\text{Fe}_{11}\text{Ti}$ at an annealing temperature of 800°C. At annealing temperatures of more than 900 °C, the H_c decreases for all alloys because of grain growth larger than the single-domain size.

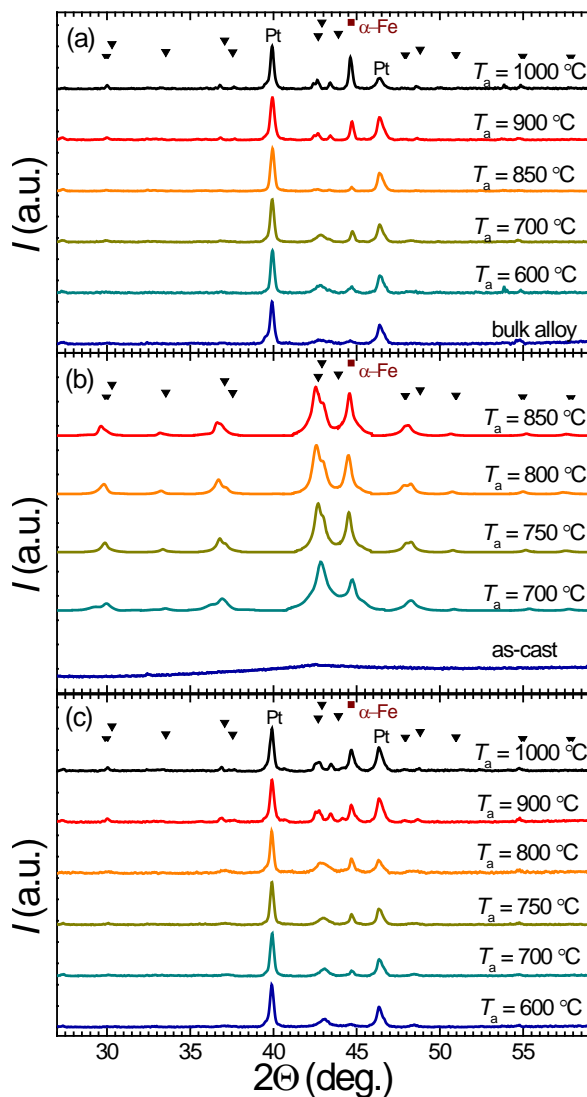


Figure 1. Normalized X-ray patterns of alloys $(\text{Sm}_{1-x}\text{Zr}_x)\text{Fe}_{11}\text{Ti}$ after different annealing temperatures, $x = 0$ (a), $x = 0.1$ (b), $x = 0.2$ (c).

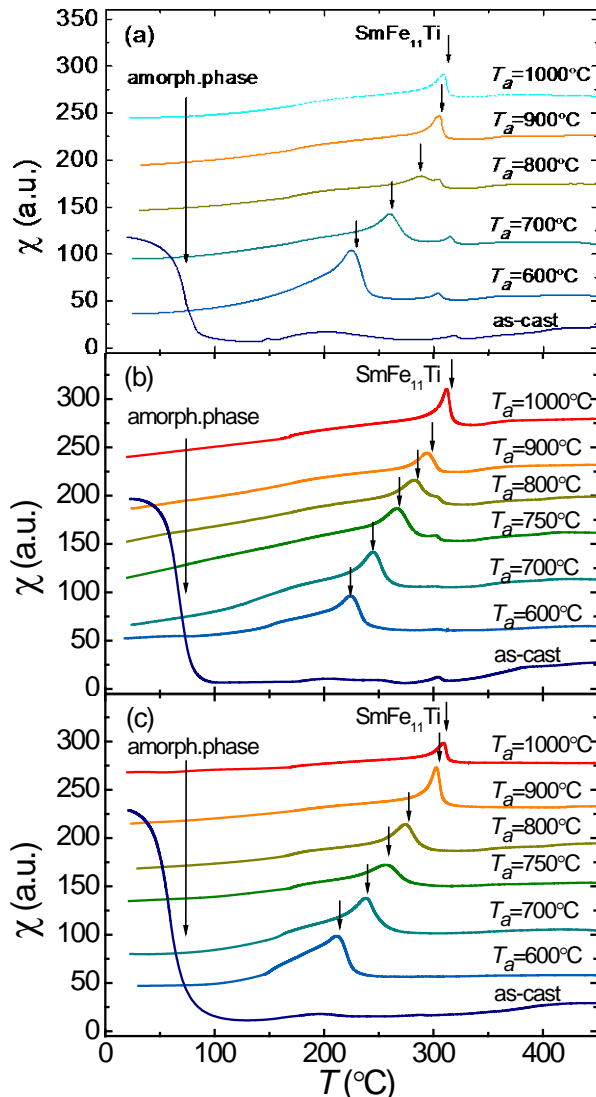


Figure 2. The initial magnetic susceptibility dependence on temperature of the alloys $(\text{Sm}_{1-x}\text{Zr}_x)\text{Fe}_{11}\text{Ti}$ after different annealing temperatures, $x = 0$ (a), $x = 0.1$ (b), $x = 0.2$ (c).

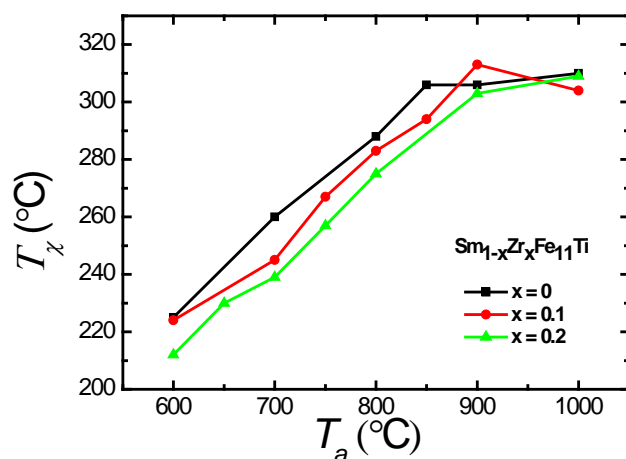


Figure 3. The position of the maximum of the magnetic susceptibility corresponding to T_C of major hard magnetic phase dependence on annealing temperature of alloys $(\text{Sm}_{1-x}\text{Zr}_x)\text{Fe}_{11}\text{Ti}$, $x = 0, 0.1, 0.2$.

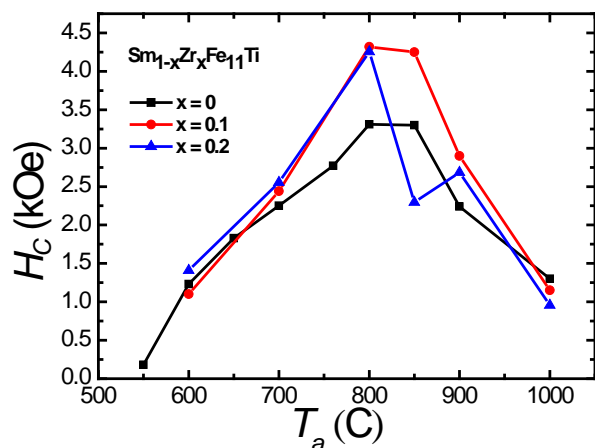


Figure 4. Dependence of the coercivity on the annealing temperature.

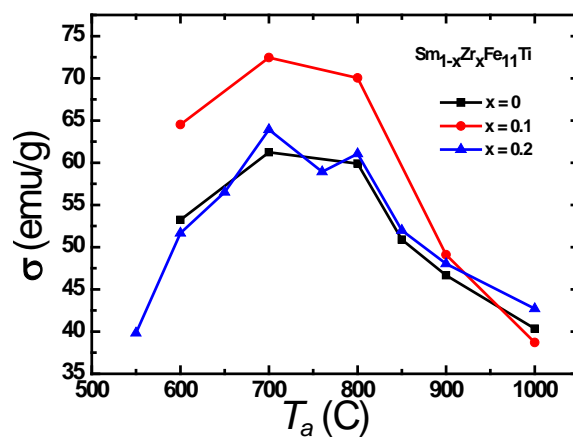


Figure 5. Dependence of the residual magnetization on the annealing temperature.

With the adding of a small amount of Zr ($\text{Sm}_{0.9}\text{Zr}_{0.1}\text{Fe}_{11}\text{Ti}$), an increase in the specific residual magnetization is observed for all annealing temperatures (Figure 5). However, the further introduction of nonmagnetic Zr leads to a decrease in the specific residual magnetization.

Figure 6 shows the hysteresis loops of the alloys $\text{SmFe}_{11}\text{Ti}$, $(\text{Sm}_{0.9}\text{Zr}_{0.1})\text{Fe}_{11}\text{Ti}$, $(\text{Sm}_{0.8}\text{Zr}_{0.2})\text{Fe}_{11}\text{Ti}$, after optimal heat treatment, 800 °C, 1 hour. The presence of a bend on the hysteresis loop suggests that in addition to the hard magnetic phase of the type ThMn_{12} there is a soft magnetic phase, for example $\alpha\text{-Fe}$ and a small amount of the amorphous phase. However, the introduction of zirconium reduces this inflection, which may indicate a change in the kinetics of the formation of $\alpha\text{-Fe}$ crystallites. The best magnetic properties are realized on the alloy $(\text{Sm}_{0.9}\text{Zr}_{0.1})\text{Fe}_{11}\text{Ti}$ after annealing at 800 °C. The specific saturation magnetization is $107 \text{ G}\cdot\text{cm}^3/\text{g}$, the specific residual magnetization in an internal magnetic field is $59.5 \text{ G}\cdot\text{cm}^3/\text{g}$, the coercivity 4.3 kOe.

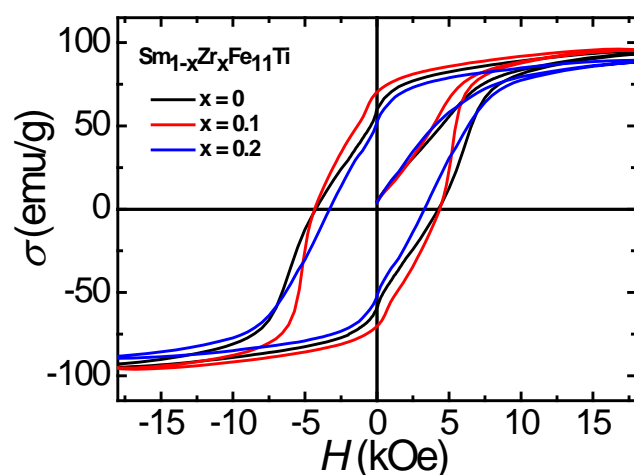


Figure 6. Limit loops after annealing at a temperature of 800°C.

4. Conclusion

In this paper, the structure and magnetic properties of samples of $(\text{Sm}_{1-x}\text{Zr}_x)\text{Fe}_{11}\text{Ti}$ alloys with $x = 0 - 0.2$, obtained by the method of fast quenching were studied. All alloys have a complex phase composition already in the initial state. Substitution a small amount of Zr ($x = 0.1$) contributes to the formation of a ThMn_{12} type phase. However, there is more intensive growth of the $\alpha\text{-Fe}$ phase grains. Substitution more Zr significantly reduces the value of the coercivity. The optimal composition and processing mode for obtaining the best magnetic properties in alloys $(\text{Sm}_{0.9}\text{Zr}_{0.1})\text{Fe}_{11}\text{Ti}$ is revealed.

Acknowledgements

The work was supported by MES of RF (contract No. 3.6121.2017/8.9) and Act 211 Government of RF (agreement No. 02.A03.21.0006).

References

- [1] De Boer F R, Huang Y K, De Mooij D B and Buschow K H J 1987 Magnetic properties of a series of novel ternary intermetallics ($RFe_{10}V_2$) *J. Less Common Metals*. **135** 199-204
- [2] De Mooij D B and Buschow K H J 1988 Some novel ternary $ThMn_{12}$ -type compounds *J. Less Common Metals*. **136** 207-15
- [3] Schultz L and Wecker J 1988 Coercivity in $ThMn_{12}$ -type magnets *J. Appl. Physics* **64** 5711-3
- [4] Gabay A M, Cabassi R, Fabbri S, Albertini F and Hadjipanayis G C 2016 Structure and permanent magnet properties of $Zr_{1-x}R_xFe_{10}Si_2$ alloys with R= Y, La, Ce, Pr and Sm *J. Alloys Compd.* **683** 271-5
- [5] De Boer F R and Buschow K H J 2003 *Physics of Magnetism and Magnetic Materials*
- [6] Hagiwara M, Sanada N and Sakurada S 2019 Structural and magnetic properties of rapidly quenched $(Sm,R)(Fe,Co)_{11.4}Ti_{0.6}$ (R=Y,Zr) with $ThMn_{12}$ structure *AIP Advances* **9** 035036
- [7] Kuno T, Suzuki S, Urushibata K, Kobayashi K, Sakuma N, Yano M, Kato A and Manabe A 2016 $(Sm,Zr)(Fe,Co)_{11.0-11.5}Ti_{1.0-0.5}$ compounds as new permanent magnet materials *AIP Advances* **6** 025221
- [8] Gabay A M and Hadjipanayis G C 2017 Mechanochemical synthesis of magnetically hard anisotropic $RFe_{10}Si_2$ powders with R representing combinations of Sm, Ce and Zr *J. Magn. Mater.* **422** 43-8
- [9] Gorbunov D I, Andreev A V, Neznakhin D S, Henriques M S, Sebek J, Skourski Y, Danis S and Wosnitza J 2018 Magnetic properties of $DyFe_{5-x}Co_xAl_7$: Suppression of exchange interactions and magnetocrystalline anisotropy by Co substitution *J. Alloys Compd.* **741** 715-22
- [10] Andreev A V, Gorbunov D I, Sebek J and Neznakhin D S 2018 Influence of Co on the magnetism of $HoFe_5Al_7$ *J. Alloys Compd.* **731** 135-42
- [11] Saito T, Miyoshi H and Nishio-Hamane D 2012 Magnetic properties of Sm-Fe-Ti nanocomposite magnets with a $ThMn_{12}$ structure *J. Alloys Compd.* **519** 144-8
- [12] Neznakhin D S, Andreev S V, Semkin M A, Selezneva N V, Volochaev M N, Bolyachkin A S, Kudrevatykh N V and Volegov A S 2019 Structure and magnetic properties of $(Sm_{0.9}Zr_{0.1})Fe_{11}Ti$ alloys with $ThMn_{12}$ -type phase *J. Magn. Mater.* **484** 212-7
- [13] Kubaschewski O 2013 *Iron-Binary phase diagrams* (Springer Science and Business Media)
- [14] Andreev A V, Bogatkin A N, Kudrevatykh N V, Sigaev S S and Tarasov E N 1989 High-Anisotropy Rare-Earth Magnets $RFe_{12-x}M_x$ *Physics of Metals and Metallography* **68** 68-75